Electron Transfer in Aromatic Solvents: The Importance of Quadrupolar Interactions

I. Read,[†] A. Napper,[†] M. B. Zimmt,*[,‡] and D. H. Waldeck*[,†]

Department of Chemistry, University of Pittsburgh, Pittsburgh, Pennsylvania 15260, and Department of Chemistry, Brown University, Providence, Rhode Island 02912

Received: May 8, 2000; In Final Form: August 1, 2000

Molecular solvation calculations are performed on a donor−bridge−acceptor (DBA) molecule in polar and nonpolar environments. A strictly dipolar treatment of solvation reproduces experimental values of the reaction free energy, $\Delta_r G$, determined in nondipolar and weakly dipolar aromatic solvents but does not simultaneously predict accurate values of $\Delta_r G$ in highly dipolar solvents. By contrast, a solvation model that includes contributions from solvent dipole and quadrupole moments (*J. Chem. Phys.* **1999**, *111*, 3630[1]) reproduces $\Delta_r G$ values over a large polarity range. The reliability of the predicted $\Delta_r G$ and solvent reorganization energies, λ_o, are assessed through fitting experimental rate data. The fits display good agreement with the experimental data and the donor−acceptor electronic couplings derived via these analyses agree with prior determinations. The availability of a model that generates reasonable predictions of $\Delta_r G$ and λ_o allows a first exploration of the temperature dependence of solvent mediated electronic coupling.

Introduction

Electron transfer between two chemical species or subunits represents a fundamental theme in many chemical transformations.[2−4] Although the understanding of electron transfer reactions has evolved considerably in the past few decades, the ability to quantify solvent effects on electron transfer rates with simple analytical models has remained elusive. Continuum models are the most widely used approaches to calculation of solvation and solvent reorganization energies.[5] This work combines recently obtained[5b,6a] electron transfer rate data over a range of solvent polarity with new data in 1,2,4-trimethylbenzene to evaluate two recently proposed molecular models for solvation and solvent reorganization energies in electron-transfer reactions.[1,7] The results demonstrate the importance of including quadrupolar interactions for the interpretation of rate data in nondipolar and weakly dipolar aromatic solvents.

In the past two decades, much of the progress toward understanding electron transfer reactions has been made in characterizing the electronic coupling between the electron donor (D) and acceptor (A) groups, and its dependence on the structural and chemical features of the system under study.[3] Donor−bridge−acceptor (DBA) systems figure prominently in these advances because of their ability to control the D/A geometry at which transfer occurs. The electron transfer rate constant's dependence on bridge length, bonding topology, state symmetry, and solvent environment have been characterized.[3,4] In systems where the D and A groups are widely separated, the (nonadiabatic) transfer is viewed as an electron tunneling event, mediated by the orbitals of the intervening atoms (or molecules). A perturbation treatment of this process, known as "superexchange",[8] successfully describes the D/A electronic interactions, whether they occur through space,[9] through covalent bridges,[4] or through solvent molecules.[6]

Recent studies from our collaboration[5b,6a,10] focus on understanding electron transfer in highly curved DBA molecules. In these molecules, solvent influences the transfer dynamics through solvation and by mediating the superexchange interaction between the D and A groups. Given tractable theories of solvation and solvent-mediated superexchange, an accurate separation of these two effects is a particular challenge. This study explores the ability of two recent molecular treatments of solvation[1,7] to reproduce the solvent's influence on the thermodynamics of electron transfer and to allow precise determination of the electronic coupling as a function of solvent and temperature. The DBA structures used in these investigations are shown in Figure 1. Each molecule consists of (1) a dimethoxyanthracene unit that acts as the electron donor upon promotion to its lowest singlet excited state, (2) a cyclobutene dicarboxylate derivative that acts as the electron acceptor, and (3) a rigid, connecting bridge. The dominant source of D/A coupling in **1** is superexchange mediated by the linear bridge.[5b,10] Thus, the solvent's primary influence on the transfer dynamics in **1** is by way of solvation. The curved bridge in **2** forms a cleft between the donor and acceptor units. The cleft is sufficiently large to accommodate a solvent molecule. The magnitude and solvent dependence of the electron-transfer rate constants in **2** demonstrate that solvents, and in particular aromatic solvents, effectively mediate the required D/A interactions.

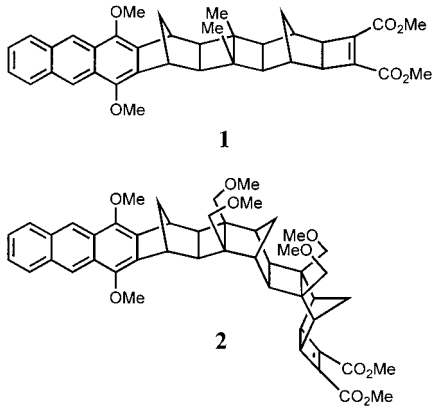

Figure 1. Molecular structure of the DBA molecules used in this work.

[†] University of Pittsburgh.
[‡] Brown University.

10.1021/jp001727c CCC: $19.00
Published on Web 09/26/2000

The rate constants obtained from these studies are interpreted through the semiclassical expression for the rate constant,[11]

$$k_{ET} = \frac{2\pi|V|^2}{\hbar\sqrt{4\lambda_o \pi k_B T}} \sum_{n=0}^{\infty} e^{-S}\left(\frac{S^n}{n!}\right) \exp\left[\frac{-(\Delta_r G + \lambda_o + nh\nu)^2}{4\lambda_o k_B T}\right] \quad (1)$$

where $\Delta_r G$ is the reaction free-energy, λ_o is the outer-sphere (solvent) reorganization energy, ν is the frequency of the effective vibrational mode, and S is the Huang−Rhys factor given as the ratio of the inner-sphere reorganization energy, λ_i to ν. This treatment assumes that the molecule's vibrational modes can be represented using a single effective high-frequency mode. The low-frequency solute and solvent vibrational modes are treated classically. The electronic coupling $|V|$ is typically estimated or calculated. A major focus of this and our previous studies is to extract the coupling magnitude from experimental rate data.

Experimental determination of each parameter ($\Delta_r G$, ν, λ_i, λ_o, $|V|$) in eq 1 is desirable, although never achieved. Typically, the effective mode frequency ν and λ_i values are determined through fitting of experimental data (such as charge-transfer spectra[12]) or are calculated quantum chemically. The value of $\Delta_r G$ is often estimated through a combination of experimental redox data and dielectric continuum corrections to the solvation energy. The outer sphere reorganization energy λ_o is usually calculated from continuum solvation theory, or in some cases may be extracted from charge-transfer spectra. A major problem with the dielectric continuum model is its failure to reproduce solvation and reorganization energies in nondipolar solvents[13] and its prediction of unreasonable temperature dependencies in highly dipolar solvents.[7] To date, molecular based models which are applicable in nondipolar or weakly dipolar solvents are unable to predict physically meaningful results in polar environments.[14] A need exists for a model capable of computing free energies and reorganization energies across a large polarity range. Once appropriate values of the four solvation and reorganization parameters are generated, the electronic coupling $|V|$ can be extracted from experimental rate data. The absolute magnitude of the calculated electronic coupling is a strong function of the parameter set used. Nonetheless, comparisons between appropriately chosen systems are robust (see ref 10 for a detailed discussion of this issue).

The reaction free energy, $\Delta_r G$, for charge separation within **2** in aromatic solvents was previously evaluated directly from the rate constants of charge separation (S1→CT) and recombination (CT→S1) that interconvert the anthracene excited state (S1) and the charge transfer state (CT).[6a] That investigation also demonstrated a very weak temperature dependence of the outer-sphere reorganization energy, λ_o.[15] In conjunction with λ_i and ν values from CT spectra and calculations,[16] it was possible to extract the electronic couplings for **2** in each solvent without the need for calculation of $\Delta_r G$ and λ_o. The experimental $\Delta_r G$ and λ_o were compared to the predictions of a molecular based solvation model that accounted for solvent molecule dipole moment and polarizability.[6a,14] This model was able to reproduce the experimentally measured $\Delta_r G$ values and predicted a reasonable temperature dependence for λ_o in a variety of alkyl substituted benzene solvents.

This work presents the application of recently developed molecular based solvation models[1,7] to the thermodynamic and rate data from **2** for a wide range of solvents and as a function of temperature. The more recently developed molecular model accounts for solvent dipole and quadrupole interactions with the solute and incorporates second-order contributions to the solvation chemical potential.[1,7] This model should provide a more realistic description of $\Delta_r G$ and λ_o as a function of solvent and temperature. This work has two goals. First, it assesses the ability of the solvation models to mimic experimentally measured reaction free energies in nondipolar and weakly dipolar solvents and predict those in highly dipolar solvents. Second, it uses the calculated reorganization energies and reaction free energies to extract the solvent dependence of the electronic coupling $|V|$. The ultimate objective is to generate a thorough understanding of solvent's roles in determining the barrier, which impedes, and the coupling, which promotes, electron transfer.

Background

A. Continuum Prediction of $\Delta_r G$ and λ_o. A crude, but often useful, treatment of the electron-transfer energetics models the solvent as a dielectric continuum. In this treatment, the donor−acceptor moieties are typically represented as individual spheres immersed in the continuum and separated by a distance, R_{cc}. $\Delta_r G$ is calculated using the Rehm−Weller equation,[17]

$$\Delta_r G = \Delta_{vac} G + \frac{e^2}{4\pi\epsilon_o}\left(\frac{1}{2r_d} + \frac{1}{2r_a} - \frac{1}{R_{cc}}\right)\left(\frac{1}{\epsilon} - 1\right) \quad (2)$$

where $\Delta_{vac} G$ is the free energy of the electron transfer in a vacuum, e is the charge on the electron, and ϵ is the solvent's static dielectric constant. r_d and r_a are the spherical radii of the donor and acceptor. Results from these calculations are used to provide a reference point for the molecular model's predictions. The solvent reorganization energy may also be calculated using continuum theory, by the relation

$$\lambda_o = \frac{e^2}{4\pi\epsilon_o}\left(\frac{1}{2r_d} + \frac{1}{2r_a} - \frac{1}{R_{cc}}\right)\left(\frac{1}{\epsilon_\infty} - \frac{1}{\epsilon}\right) \quad (3)$$

where ϵ_∞ is the high-frequency dielectric constant, taken to be the square of the solvent's refractive index.

B. Molecular Model for $\Delta_r G$. In earlier work, a dipolar, polarizable hard sphere model for the solvent was used to compute both $\Delta_r G(T)$ and $\lambda_o(T)$ for **2** in weakly dipolar aromatic solvents.[6a,14] The model treated the solute as a polarizable sphere with different permanent dipole moments for the locally excited and charge transfer states. The model was developed particularly for application to weakly dipolar systems and is expected to fail in highly dipolar solvents since solute−solvent-solvent correlations are neglected. The present investigation uses a more sophisticated treatment of the solute−solvent interactions and compares two separate approaches to the modeling. First, the $\Delta_r G$ values are computed using a revised dipolar, polarizable model.[7] This treatment includes higher order contributions to the solvation energy, thus providing a more accurate description of solvation in highly dipolar solvents. Second, a solvation model that also explicitly incorporates quadrupolar interactions is used to compute the solvation energies.[1] In both cases, the gas phase solvent dipole moments are renormalized to account for inductive dipolar and quadrupolar (when relevant) interactions with the surrounding solvent. This renormalization procedure is outlined by Gray and Gubbins.[18]

Matyushov[1] calculates $\Delta_r G$ as the sum of four contributions,

$$\Delta_r G = \Delta_{vac} G + \Delta_{dq,i} G^{(1)} + \Delta_{disp} G + \Delta_i G^{(2)} \quad (4)$$

where $\Delta_{vac} G$ is the free energy of the process in a vacuum, $\Delta_{dq,i} G^{(1)}$ is the contribution from first-order dipole, quadrupole,

and induction interactions, $\Delta_{disp}G$ is the contribution from dispersion interactions and $\Delta_i G^{(2)}$ is the contribution from second-order induction interactions. The $\Delta_{dq,i}G^{(1)}$ term includes dipole−dipole and dipole−quadrupole interactions between the solute dipole and the solvent electric moments and includes the induction interactions that arise from the polarizability of both the solute and solvent. It is calculated through the relationship

$$\Delta_{dq,i}G^{(1)} = -\frac{(m_e^2 - m_g^2)}{R_{eff}^3} f(y_d, y_q)\, \Psi^P(y_d, y_q) \qquad (5)$$

where m_e is the solute dipole moment of the charge transfer state, and m_g is the reactant state dipole moment. The function $f(y_d, y_q)$ renormalizes the solute dipole moment to account for its size and polarizability. It is given by

$$f(y_d, y_q) = \left[1 - \frac{2\alpha_0}{R_{eff}^3}\Psi^P(y_d, y_q)\right]^{-1} \qquad (6)$$

Here α_o is the solute polarizability and $\Psi^P(y_d, y_q)$ is referred to as the "polarity response function". R_{eff} represents the effective radius of a spherical dipolar solute. It accounts for the local packing of solvent molecules against the solute sphere and is determined through the solute−solvent hard sphere pair distribution function $g_{0s}^{(0)}(r)$, namely

$$\frac{1}{R_{eff}^3} = 3\int_0^\infty \frac{dr}{r^4} g_{0s}^{(0)}(r) \qquad (7)$$

Matyushov evaluated the integral numerically and fit it to the following polynomial form; i.e.

$$\frac{1}{R_{eff}^3} = \frac{I_{0s}^{(2)}}{\sigma^3} \qquad (8)$$

The form of the $I_{0s}^{(2)}$ is given explicitly in the Appendix. The polarity response function, $\Psi^P(y_d, y_q)$, is written in terms of the reduced dipolar density, y_d, the quadrupolar density, y_q, and the solute−solvent perturbation integrals. The densities are computed using the relations

$$y_d = \frac{4\pi}{9}\frac{\rho}{kT}m'^2 + \frac{4\pi}{3}\rho\alpha \qquad (9a)$$

$$y_q = \frac{2\pi}{5}\frac{\rho}{\sigma^2 kT}Q^2 \qquad (9b)$$

where Q is the average quadrupole moment (Table 2), m' is the renormalized solvent dipole moment,[1,7] ρ is the solvent number density, α is the solvent polarizability, and σ is the solvent hard sphere diameter. Matyushov[1,7] has shown that the perturbation integrals are well represented by a polynomial interpolation and writes $\Psi^P(y_d, y_q)$ as

$$\Psi^P(y_d, y_q) = \frac{\dfrac{y_d I_{0s}^{(2)} + y_q I_6^{(2)}}{I_{0s}^{(2)}}}{1 + \dfrac{y_d^2\kappa_d I_{0s}^{(3)} + y_d y_q \kappa_{dq} I_{DDQ}^{(3)} + y_q^2 \kappa_q I_{DQQ}^{(3)}}{y_d I_{0s}^{(2)} + y_q I_6^{(2)}}} \qquad (10)$$

The explicit form of the polynomial interpolation for the two- and three-particle perturbation integrals ($I^{(2)}$, $I^{(3)}$) are written in the Appendix.[19] The κ_i parameters correct for saturation of the solvent response that arises from three particle (solute−solvent−solvent) correlations.[1] These factors depend on the ratio of solute−solvent diameters, $d = 2R_o/\sigma$, through the relations,

$$\kappa_d = 1 + \left[\frac{d}{(d+1)}\right]^2 \qquad \kappa_q = 2 + \frac{1}{(d^5+2)}$$

$$\kappa_{dq} = 2 - \frac{d^5}{(d^5+2)}$$

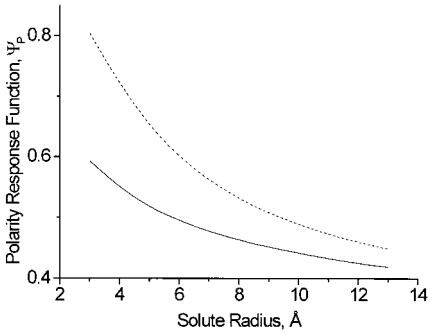

Figure 2. Behavior of the polarity response function for the dipole (solid line, $\langle Q\rangle = 0$ D Å) and dipole−quadrupole (dashed line, $\langle Q\rangle =$ 3 D Å) models are shown as a function of the solute radius.

Figure 2 shows the dependence of the response function (eq 10) on the effective solute radius, R_o, for the dipole model ($Q = 0$, solid line) and the dipole−quadrupole model ($Q = 3.0$ D Å, dashed line). These calculations were performed using constant values for the solvent hard sphere diameter (5 Å), solvent polarizability (10 Å^3), and dipole moment (2 D). The solute polarizability and dipole moment were chosen to be 70 Å^3 and 34 D, respectively. In both models, the magnitude of the calculated response function decreases with increasing solute radius. According to eq 5, the predicted free energies become more negative as the size of the solute decreases. Figure 2 also shows that inclusion of quadrupolar interactions increases the magnitude of the polarity response function. This behavior indicates that quadrupolar interactions are stabilizing, and that their inclusion will require a larger solute radius, relative to the dipolar model, to reproduce a given value of the reaction free energy, $\Delta_r G$.

Second-order induction interactions of the solute dipole with the solvent molecules are accounted for by the $\Delta_i G^{(2)}$ term. These interactions arise from correlations of polarization fluctuations generated by the solvent's induced dipoles.[7] Matyushov relates these interactions to the solvent polarizability and the high-frequency dielectric constant, ϵ_∞, and writes,

$$\Delta_i G^{(2)} = -(m_e^4 - m_g^4)\, f(y_e)\frac{1}{200\pi\rho kT}\frac{(\epsilon_\infty - 1)^2}{(\epsilon_\infty + 2)^2} \times [9 + 8(\epsilon_\infty - 1)^2]I_{0s}^{(4)} \qquad (11)$$

where the quantity $y_e = (4\pi/3)\,\rho\alpha$ is the reduced polarizability density of the solvent. The function $f(y_e)$ renormalizes the solute dipole by the polarizability response of the solvent. Its value is calculated using

$$f(y_e) = \left[1 - \frac{2\alpha_0}{R_{eff}^3}\Psi^P(y_e)\right]^{-1} \qquad (12)$$

The polarizability response function, $\Psi^P(y_e)$, is given by

$$\Psi^{P}(y_e) = \frac{y_e}{1 + \kappa_d y_e I^{(3)}_{0s}/I^{(2)}_{0s}} \quad (13)$$

Note that eq 13 is derived directly from the polarity response function (eq 10). When the solvent has no permanent dipole or quadrupole moment, the polarizability response function of the fluid is given by this term.

The dispersion contribution, $\Delta_{disp}G$, has a relatively small effect on the overall free energy (see Table 7). Its value can be calculated from the solvent−solvent Lennard-Jones energy, ϵ_{LJ}, and the solvent hard sphere diameter σ. These parameters were obtained through the additivity method described by Ben-Amotz.[20] $\Delta_{disp}G$ is given by

$$\Delta_{disp}G = -\frac{\Delta\gamma'}{\alpha_s} 8\eta\epsilon_{LJ}\left(\frac{\sigma}{R_{eff}}\right)^3 \quad (14)$$

where η is the reduced packing density, defined as $(\pi/6)\rho\sigma^3$, and α_s is the solvent polarizability. The parameter $\Delta\gamma'$ is determined by

$$\Delta\gamma' = \Delta\alpha_o \frac{2I_o}{I_o + I_s} \quad (15)$$

where $\Delta\alpha_o$ is the change in polarizability between the locally excited state and the charge transfer state of the solute, I_o is the ionization potential of the solute and I_s is the ionization potential of the solvent. $\Delta\gamma'$ is one of three adjustable parameters determined by a simultaneous fit of the experimental Δ_rG values measured as a function of temperature in all of the alkylated benzene solvents (The best fit values are reported in Table 1.) Values for the individual contributions to Δ_rG are listed in Table 7.

C. Molecular Model for the Reorganization Energy, λ_o. The same polarizable hard-sphere model[1] is used to compute the reorganization energy λ_o. The reorganization energy is written as a sum of three components $\lambda_o = \lambda_p + \lambda_{ind} + \lambda_{disp}$, where λ_p accounts for solvent reorganization arising from the solvent dipole and quadrupole moments, λ_{ind} is the contribution from induction forces and λ_{disp} accounts for the dispersion interactions. An expression for λ_p was derived using the linear response approximation for the chemical potential,[14] so that

$$\lambda_p = \frac{(m_e - m_g)^2}{R_{eff}{}^3}[f(y_d, y_q)\,\Psi^{P}(y_d, y_q) - f(y_e)\,\Psi^{P}(y_e)] \quad (16)$$

where $\Psi^{P}(y_d, y_q)$ is given by eq 10 and $\Psi^{P}(y_e)$ is given by eq 13. This contribution accounts for the reequilibration of the solvent's nuclear modes to the newly formed electronic configuration of the charge transfer state. Although the induction forces make a relatively small contribution to the overall reorganization energy in highly polar solvents, in weakly polar systems the dipolar contributions are small and induction interactions are significant. According to ref 7, the induction term can be calculated through,

$$\lambda_{ind} = \frac{(m_e{}^2 - m_g{}^2)^2 f(y_e)^2}{kT400\eta\sigma^6}\frac{(\epsilon_\infty - 1)^2}{(\epsilon_\infty + 2)^2}\left[3 + \frac{8}{3}(\epsilon_\infty - 1)^2\right] I^{(4)}_{0s} \quad (17)$$

The polynomial form of the two-particle perturbation integral $I^{(4)}{}_{0s}$, is given in the Appendix. The contribution from the dispersion forces is expected to be small in both dipolar and nondipolar solvents and in most cases these energies can be neglected. However, they can become significant if the solvent diameter and density is large. Matyushov defines λ_{disp}[21] as a second-order perturbation over the solute−solvent dispersion potential so that

$$\lambda_{disp} = \frac{\Delta\gamma'^2}{\alpha_s{}^2}\frac{8\eta}{3}\beta\epsilon_{LJ}{}^2 J_1(\rho^*, r_{0s}) \quad (18)$$

The polynomial form of the integral J_1 is given in the Appendix along with the calculated values of λ_o, λ_p, λ_{disp}, and λ_{ind} predicted by the two treatments.[22]

TABLE 1: Best Fit Parameters Used in Δ_rG Calibrations

	model		
	dipole	dipole−quadrupole	lit.[a]
solute radius (Å)	6.19	7.25	
$\Delta_{vac}G$ (eV)	0.326	0.340	
$\Delta\gamma'$ (Å^3)	−9.5	1.7	
	Solvent Polarizability (Å^3)		
benzene	10.3	9.5	10.0
toluene	11.8	10.9	11.8
cumene	15.5	16.3	16.0
mesitylene	15.2	14.8	15.5
TMB[b]	14.6	15.5	
TIP[c]	26.9	31.7	31.8[d]

[a] Literature values obtained from *CRC Handbook*, 78th ed.; CRC Press: Boca Raton, FL, 1998. [b] TMB is 1,2,4-trimethylbenzene. [c] TIP is 1,3,5-triisopropylbenzene. [d] Literature value could not be found. Value listed is for 1,3,5-tri-*tert*-butylbenzene.

Results and Discussion

A. Calculation of Δ_rG. Simulation of the Δ_rG values using the molecular model requires determination of three parameters: $\Delta_{vac}G$, the solute radius R_o, and $\Delta\gamma'$. The Δ_rG values for **2** in every solvent (benzene, toluene, cumene, mesitylene, 1,2,4-trimethylbenzene (TMB), and triisopropylbenzene (TIP)) and temperature were fit, simultaneously, to eq 4 using Microsoft Excel 97 on a Pentium based PC. The solvent dipole and quadrupole moments were calculated at the RHF/6-31G**// RHF/6-31G** level of theory using Gaussian 98[23] on a Silicon Graphics Power Indigo workstation (Tables 2 and 3). The effective quadrupole moment $\langle Q\rangle$ reported in Table 3 was used in the calculations. This effective quadrupole gives exact results for axially symmetric quadrupole tensors and is correct through second order for nonaxially symmetric quadrupole tensors. With the exception of benzonitrile, the quadrupole tensors of the investigated solvents are axially symmetric, or nearly so. The dipole moment of the anthracene excited state was set to 0 D and the dipole moment of the charge separated state was calculated to be 34 D.[24] In previous work, the solute polarizability was estimated as 100 Å^3, but recent calculations (RHF/6-31+G(d)) suggest that this value is too high and a solute ground-state polarizability of 70 Å^3 was used. After initial values of the three parameters were determined, the literature value of the solvent's polarizability was adjusted (<10%) to improve the fits (see Table 1). The solvent parameters used in the calculations are given in Tables 1−3.

Figure 3 presents the fits of the two models to the experimental Δ_rG data, and Table 1 presents the parameter set for each fit. It is clear from the plots that both models can reproduce the data in nondipolar solvents but they predict very different Δ_rG values in highly dipolar solvents. In the nitrile solvents the $S_1 \leftrightarrow$ CT equilibrium was not measurable. As a result a

TABLE 2: Solvent Parameters Used in Matyushov Modeling[a]

solvent	m[b] (D)	σ[c] (Å)	ϵ_{LJ}[d] (K)	η[e]
benzene	0	5.28	544	0.520
toluene	0.29	5.68	603	0.543
cumene	0.25	6.29	679	0.561
mesitylene	0.07	6.40	720	0.593
TMB	0.30	6.31	720	0.579
TIP	0.08	7.40	949	0.552
acetonitrile	4.06	4.14	405	0.425
benzonitrile	4.2	5.68	698	0.562

[a] TMB is 1,2,4-trimethylbenzene. TIP is 1,3,5-triisopropylbenzene. [b] The vacuum dipole moment. [c] The hard sphere solvent diameter. [d] The Lennard-Jones energy parameter. [e] The packing fraction at 295 K.

TABLE 3: Diagonal Quadrupole Moment Tensor Components Used To Compute $\langle Q \rangle$[a]

solvent	Q_{xx} (D Å)	Q_{yy} (D Å)	Q_{zz} (D Å)	$\langle Q \rangle$ (D Å)
benzene	4.146	4.146	−8.288	8.288
toluene	4.122	4.122	−7.893	7.896
cumene	3.624	4.206	−7.830	7.836
mesitylene	3.954	3.519	−7.464	7.467
TIP	2.848	4.835	−7.683	7.770
TMB	4.209	3.088	−7.299	7.326
acetonitrile	−3.369	1.685	1.685	3.369
benzonitrile	−12.61	13.82	−1.214	15.39

[a] TMB is 1,2,4-trimethylbenzene. TIP is 1,3,5-triisopropylbenzene. $\langle Q \rangle = |\sqrt{^2/_3 \sum Q_{ii}^2}|$.

comparison of calculated and experimental $\Delta_r G$ values is not possible. The best fit value of the solute radius in the dipole−quadrupole model, 7.25 Å, is considerably larger than in the dipole analysis, 6.19 Å. This difference is consistent with the larger polarity response function and increased stabilization energy predicted by the model that includes solvent quadrupoles (Figure 2). AM1 calculations of **2** indicate that a sphere of ∼7.0 Å is required to fully encapsulate the solute. This result is consistent with the best fit solute radius found using the dipole−quadrupole model. The best fit $\Delta\gamma'$ was found to be ∼−9.5 Å^3 for the dipole model and 1.7 Å^3 for the dipole−quadrupole model. In both cases, the small size of $\Delta\gamma'$ suggests similar polarizabilities for the LE and CT states. In the dipole−quadrupole model the dispersion makes a neglible contribution to the reaction free energy. In the dipole model the dispersion term plays a significant role in determining the proper ordering of $\Delta_r G$ with solvent. Quantum chemical calculations of $\Delta_{vac} G$ were performed using the vacuum ionization potentials and electron affinities of the donor−acceptor pair. The results predict that $\Delta_{vac} G$ is ∼1.1 ± 1.0 eV. Table 1 shows that the best fit value for each model lies within the uncertainty limit of the calculation. Since the values of $\Delta_{vac} G$ for each model are similar, their absolute magnitude is not expected to effect the overall results. Among the three fit parameters, variation of the solute hard sphere radius, R_o, between the values determined in the two models, exerts the greatest impact on the fitting results.

Figure 3 shows that both molecular approaches accurately reproduce the observed free energies in nondipolar and weakly dipolar solvents. Because of model specific differences in the best fit solute parameters, the predicted $\Delta_r G$ values are strikingly different in the nitrile solvents. The dipolar model predicts a free energy of −1.47 eV in acetonitrile and −1.57 eV in benzonitrile at 300 K, whereas the dipole−quadrupole model predicts a $\Delta_r G$ of −0.71 eV in acetonitrile and −0.88 eV in benzonitrile. It is evident that use of the dipole−quadrupole model leads to significantly smaller estimates of the reaction

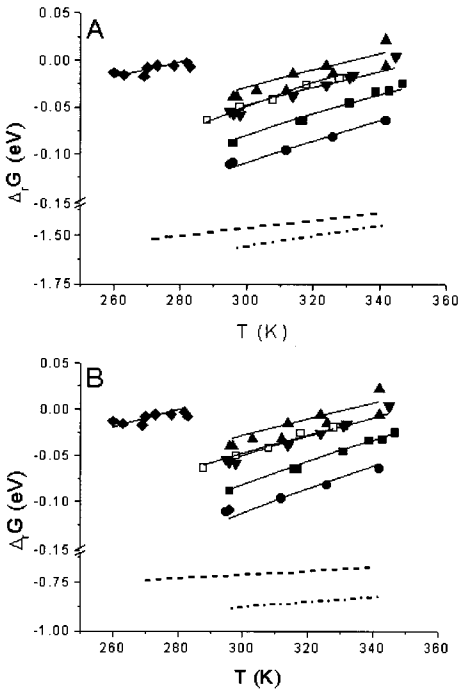

Figure 3. The lines show the temperature-dependent free energies calculated using the dipole model in panel A and the dipole−quadrupole model in Panel B. The solid lines show the predicted free energies in alkylbenzenes, the dashed line shows the predicted free energy in acetonitrile and the dashed−dotted line shows the predicted free energy in benzonitrile. Experimental data is shown for benzene (●), toluene (■), cumene(▼), mesitylene (▲), TMB (□) and TIP (◆). Note that the *y*-axis is broken in both plots.

exoergocity in polar solvents. The experimental redox potentials in acetonitrile place the energy of the infinitely separated D^+ and A^- ions −0.51 eV below the energy of the anthracene excited state.[16] Use of continuum models for Coulomb attraction and solvation corrections (eq 2) suggest the $\Delta_r G$ values are −0.56 eV in acetonitrile and −0.53 eV in benzonitrile (Table 4). These comparisons indicate that the dipole model predicts unrealistically negative $\Delta_r G$ values in both of the nitrile solvents. The inclusion of quadrupole moments when fitting the data in the nondipolar and weakly dipolar aromatic solvents provides more realistic solute parameters and generates more reasonable $\Delta_r G$ values across a wider range of polarity. The dipole−quadrupole model's prediction of a more negative $\Delta_r G$ in benzonitrile than in acetonitrile arises from the difference in their quadrupole moments and warrants comment. The model[1] assumes that the dipole moment vector and the principal axis of the quadrupole tensor are collinear, which is incorrect for benzonitrile. Since the quadrupole tensor of benzonitrile is nonaxial, corrections beyond second order may be important.[25] As a result the sum of the two solvation contributions may be less effective than that predicted by the model.

For the dipole model, the dipolar density, y_d, is the primary solvent parameter controlling the magnitude of the polarity response function. It accounts for interactions involving the solvent permanent dipole and the solvent polarizability (eq 9a). Many of the aromatic solvents employed in this investigation possess small (or zero) permanent dipole moments; thus the stabilization energy from induction forces dominates $\Delta_r G$. Since these interactions are small, the experimental free energies and their temperature dependencies are reproduced by decreasing the solute radius, which enhances the solvent's polarity response function, $\Psi^P(y_d, 0)$. Although the required, best fit solute radius is clearly too small, one obtains a reasonable fit to the data in

TABLE 4: Experimental and Calculated $\Delta_r G$ (eV) at 295 K[a]

		model		
	expt	dipole	dipole−quadrupole	continuum
benzene	−0.109	−0.112	−0.115	−0.072
toluene	−0.089	−0.086	−0.083	−0.094
cumene	−0.058	−0.054	−0.051	−0.094
mesitylene	−0.039	−0.033	−0.032	−0.070
TMB	−0.064	−0.062	−0.057	−0.060
TIP[b]	−0.013	−0.020	−0.018	−0.070
acetonitrile		−1.467	−0.713	−0.560
benzonitrile		−1.570	−0.882	−0.530

[a] TMB is 1,2,4-trimethylbenzene. TIP is 1,3,5-triisopropylbenzene. [b] Results tabulated at 282 K.

a similar set of solvents, such as the alkylbenzenes. However, in those solvents where the polarity response function is dominated by permanent dipole moments, as in acetonitrile and benzonitrile, the small cavity radius predicts unrealistically large solvation energies. The small differences between the predicted $\Delta_r G$ values in acetonitrile and benzonitrile result from their different polarizabilities.

Inclusion of quadrupole solvation provides a more realistic description of the intermolecular forces experienced by the solute in aromatic solvents. The best fit solute radius is larger than that found with the dipole model and is in reasonable agreement with the molecule's van der Waals radius. The $\Delta_r G$ values calculated using the dipole−quadrupole model are shown in Figure 3B. (The dipole−quadrupole polarity response function (eq 10) includes both y_d and y_q.) For the nondipolar and weakly dipolar aromatic solvents, y_q and y_d are comparable, so that one observes a large increase in the stabilization energy for the quadrupole model compared to the dipole model. This produces a 1.1 Å increase in the best fit solute radius compared to the dipole only model. As a result, the $\Delta_r G$ values in the nitrile solvents are markedly different from those calculated when the quadrupole terms are not included (see Table 4). This change reflects the decreased solvation provided by the dipole density for larger R_o values. Because the quadrupolar density makes only a small contribution to the polarity response function in acetonitrile, the $\Delta_r G$ value is largely determined by dipole interactions.

The results show that the dipole−quadrupole model can predict reasonable $\Delta_r G$ values across a wide range of polarity. For comparison, calculations of $\Delta_r G$ using continuum theory are presented in Table 4. The results show that these solvents can be divided into three groups: nondipolar (benzene, mesitylene, TIP), weakly dipolar (toluene, cumene), and highly dipolar (acetonitrile, benzonitrile). In each group, the continuum estimates are identical: −0.07 (nondipolar), −0.094 (weakly dipolar), and ∼−0.54 (highly dipolar). As expected, these results do not agree with experiment. The value of $\Delta_r G$ in the alkylated benzene solvents are determined primarily by the size of the solvent molecules (an observation consistent with the solvents ability to pack against the solute). For the nitrile solvents, exact experimental data is not available, but because the quadrupole moment of acetonitrile is significantly smaller than benzonitrile, one expects different $\Delta_r G$ values in these two solvents. In addition, the continuum model overestimates the stabilization energy of the weakly dipolar solvents toluene and cumene. These findings confirm the inability of the continuum model to reproduce the experimentally determined $\Delta_r G$ values.

B. Calculation of the Reorganization Energy. Table 7 presents the calculated λ_o values from both models and list the individual contributions to the reorganization energy as a function of temperature. Although the calculated λ_o are physically reasonable, it is difficult to assess their accuracy as very little experimental data is available for λ_o. In the nondipolar and weakly dipolar solvents, the dipole only model predicts λ_{ind} to be the dominant contributor to the overall reorganization energy. In contrast, when the quadrupole moments are included, λ_p is the dominant term in every solvent. This result can be understood in terms of the dipole and quadrupole densities. In the dipole model, dipolar and polarization interactions contribute to the polarity response function of the fluid. For a nondipolar solvent, $\Psi^p(y_d, 0)$ and $f(y_d, 0)$ reduce to $\Psi^p(y_e)$ and $f(y_e)$, respectively. The two terms in eq 16 cancel and λ_p is zero. If the solvent molecule possesses a dipole moment, the dipolar density increases to a value greater than the polarizability density, y_e. In highly polar solvent, e.g., nitriles, the dipole contribution dominates. In the dipole−quadrupole model, λ_p contains an additional contribution from the quadrupole density, y_q. Because the quadrupole density exceeds the polarizability density in every solvent, λ_p always makes the dominant contribution to the overall reorganization energy. The best fit solute radius is larger when quadrupole moments are included in the data fitting; thus contributions from induction forces are reduced compared to those in the dipole model. Both the dipole and dipole−quadrupole models suggest that λ_o decreases with increasing temperature in all solvents. This prediction agrees with experimental results.[7,26] By contrast, the continuum model predicts that λ_o increases with temperature in highly dipolar solvents.

Dispersion interactions make negligible contributions to λ_o in highly dipolar solvents but increase in importance as the polarity of the solvent decreases. According to eq 18, λ_{disp} depends quadratically on the Lennard-Jones energy ϵ_{LJ} (the magnitude of which is correlated to the size and number of substituents on the aromatic ring[20]) and the reduced packing density, η. The dipole model predicts significant λ_{disp} values in the nondipolar aromatic systems because of the increased contribution from the perturbation integral, J_1. This contribution is less significant for larger values of R_o. As a result, the dipole−quadrupole model predicts negligible values for λ_{disp} in every solvent.

C. Fitting the Rate Constants. With values for λ_i, ν, λ_o, and $\Delta_r G$, it is possible to fit the experimentally determined electron-transfer rate data to the semiclassical rate equation and to determine the electronic coupling, $|V|$. As discussed elsewhere for **2**,[10] λ_i was taken to be 0.39 eV and ν was taken to be 1410 cm^{-1}. The rate constants were fit using the results from both the dipole and the dipole−quadrupole model. As found previously,[6a] attempts to reproduce the observed rate constants using the λ_o predicted by the models and a constant $|V|$ were not entirely successful. The solid lines in Figure 4 show the predicted temperature dependence of the electron-transfer rate constants in the nitrile solvents. These curves were obtained using the $\Delta_r G$ and λ_o derived from the dipole−quadrupole model and a temperature independent value of $|V|$. Clearly, the fits are poor. The dashed lines represent fits in which $|V|$ and $\lambda_o(295)$ are treated as adjustable parameters. The temperature dependence of the reorganization energy was predicted by the dipole−quadrupole model. These fits are excellent and predict electronic couplings of 27 cm^{-1} in acetonitrile and 93 cm^{-1} in benzonitrile. These values agree well with those found from an earlier continuum treatment,[5b] but are 4−5-fold larger than values predicted using an alternate ion pair solvation model.[10]

Two different approaches were taken to fit the data in the alkylated aromatic solvents. In the first approach, the $\Delta_r G$ and

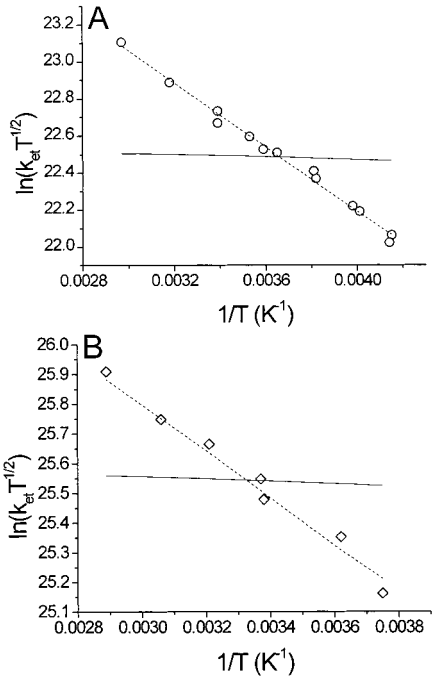

Figure 4. Experimental rate data is shown for acetonitrile (○, Panel A) and benzonitrile (◇, Panel B). The solid lines represent fits using the free energy and reorganization energy calculated using the dipole−quadrupole model. The dashed lines represent the calculated rate constants when the free energies and the temperature dependence of λ_o was calculated using the dipole−quadrupole model but $\lambda_o(295)$ was varied.

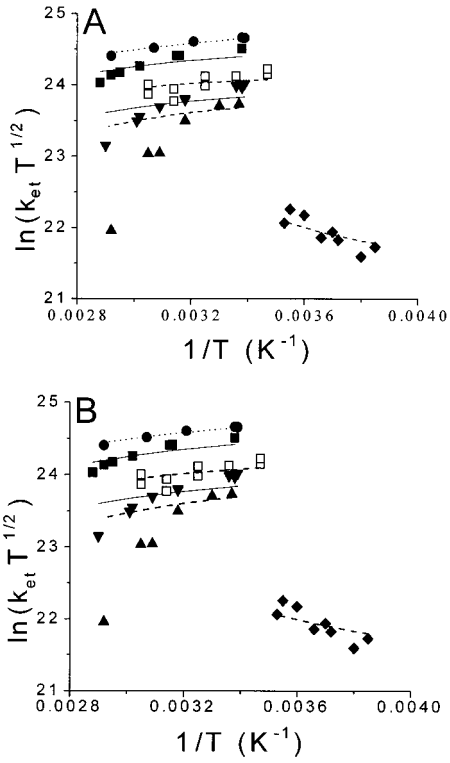

Figure 5. Experimental rate data (k_{et}) are shown for benzene (●), toluene (■), cumene(▼), mesitylene(▲), TMB (□), and TIP (◆). Panel A shows the fits using the free energy and temperature dependence of the outer sphere reorganization energy predicted by the dipole model. Panel B shows the fits using the energies predicted by the dipole−quadrupole model. The dotted curve shows the fit for the benzene data, the solid curve shows the fits for the singly substituted benzenes (toluene and cumene), and the dashed curves show the fits for the triply substituted benzenes (mesitylene, 1,2,4-trimethylbenzene, TIP). In each case, the electronic coupling and reorganization energy at 295 K were fitting parameters.

$d\lambda_o/dT$ were taken from the model. Both $|V|$ (assumed temperature independent) and $\lambda_o(295)$ were allowed to vary in each solvent. The fits to the rate constant data for the alkylated benzene solvents are shown as a function of temperature in Figure 5 for the dipole model (panel A) and the dipole−quadrupole model (panel B). In every case, the sum of eq 1 was evaluated through the sixth term. The best fit parameters obtained from each method are summarized in Table 5. In the second approach, it was assumed that the $\Delta_r G$ and λ_o values predicted by the dipole−quadrupole model are accurate and the electronic coupling was treated as both solvent and temperature dependent. The results of this analysis are shown in Figure 6.

In the first approach, fitting the rate constant data (Figures 4 and 5) provides values for the electronic coupling and the room temperature reorganization energy as a function of solvent (see Table 5). The electronic coupling decreases monotonically as the alkyl substitution on the phenyl ring increases for both models. As discussed elsewhere,[6a] this trend results from increased steric bulk of the solvent molecules inhibiting access of the aromatic core to the molecular cleft between the donor and acceptor groups. This results in decreased through solvent coupling. The magnitudes of the coupling elements are slightly different from those reported earlier. In cumene and mesitylene, a decreased quality of the fitted curves is observed. There are several possible explanations for the effect. First, the temperature dependence of λ_o calculated by the molecular models may be too steep. The fits to the data using a constant λ_o are significantly better than those shown here. However, this explanation cannot explain the particularly steep decrease of the rate constant in mesitylene with increasing temperature. Second, both models predict a quasi-linear temperature dependence for λ_o which may not be accurate in these solvent systems. If the equilibrium between solvent bound and solvent unbound "clefts" changes significantly through this temperature range, nonlinear changes in λ_o and $|V|$ with temperature would be expected. We are currently exploring the origin of these steep drops in rate with temperature in the bulkier aromatic solvents.

TABLE 5: Regression Estimates of the Electronic Couplings and Reorganization Energies Obtained Using the Matyushov Solvation Model[a]

	model			
	dipole		dipole−quadrupole	
solvent	$\|V\|$ (cm^{-1})	$\lambda_o(295)$ (eV)	$\|V\|$ (cm^{-1})	$\lambda_o(295)$ (eV)
benzene	9.47	0.239	10.1	0.258
toluene	8.84	0.220	8.93	0.217
cumene	6.70	0.180	6.33	0.167
mesitylene	6.12	0.152	5.91	0.144
TMB	7.99	0.189	6.98	0.162
TIP	1.03	0.001	1.09	0.009
acetonitrile	31.6	2.51	27.7	1.49
benzonitrile	116.7	2.60	92.7	1.67

[a] TMB is 1,2,4-trimethylbenzene. TIP is 1,3,5-triisopropylbenzene.

The second approach to fitting the rate data hypothesizes that the electronic coupling is temperature dependent. In this approach, the values of $\Delta_r G$ and λ_o predicted by the dipole−quadrupole model (see Table 7) were used, and the value of $|V|$ at each temperature was derived from the experimental rate constants. Figure 6 shows a plot of the electronic couplings as a function of temperature. It is clear from the plot that solvents in which an aromatic core can access the cleft display the largest

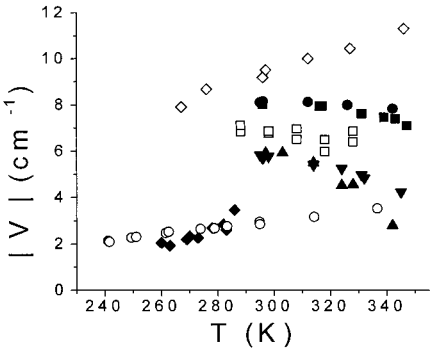

Figure 6. Temperature-dependent electronic couplings are shown. These values are calculated from eq 1 using the absolute $\Delta_r G$ and λ_o values from the dipole−quadrupole model. Data are shown for benzene (●), toluene (■), cumene (▼), mesitylene (▲), TMB (□), TIP (◆), acetonitrile (○), and benzonitrile (◇).

electronic couplings. In the nondipolar and weakly dipolar aromatic solvents (other than TIP), the coupling displays a systematic but small decrease as the temperature increases (resulting in a predicted decrease of rate by 10−60% over a 40 to 50 K temperature range). To speculate, this behavior could indicate a shift in the distribution of solvent-bound and solvent-unbound DBA "clefts" in solution. With increasing temperature, the population of unbound "clefts" increases and the ensemble averaged value of the electronic coupling decreases because the solvent-unbound structure lacks the through solvent coupling pathway. This trend is correlated to solvent size and is most apparent in cumene and mesitylene. The triisopropyl solvent exhibits the opposite behavior; i.e., the coupling increases as the temperature increases. Previously, it was demonstrated that this solvent experiences a large energy barrier to placement of its aromatic core within the cleft, between the D and A groups. Higher temperatures may increase the probability of placing the solvent's aromatic core between the D and A groups. In the polar solvents, the coupling increases with temperature also, enhancing the rate constant by 1.5−3-fold. While this approach to fitting the rate data provides stimulating conjecture into the temperature dependence of the electronic coupling, the observed changes may result from systematic errors in the determination of $\Delta_r G$ and/or λ_o. More experimental work is necessary before a reliable conclusion can be reached.

Conclusions

Measurement of $\Delta_r G$ and rate constants for electron transfer in highly dipolar, weakly dipolar and nondipolar solvents were used to evaluate two molecular models of solvation. The analysis shows that quadrupolar interactions must be included when computing solvation energies in nondipolar and weakly dipolar aromatic solvents. The quadrupole model was shown to accurately reproduce experimental free energy data and to make reasonable predictions of these energies in the polar solvents acetonitrile and benzonitrile. The analysis shows that λ_{disp} is inconsequential and may be ignored. In addition, the quadrupole model was able to produce physically reasonable values of λ_o. Two separate approaches were used to fit the experimental rate constants. First, the calculated temperature dependence of λ_o was used, and the electronic coupling and λ_o at 295 K were treated as adjustable parameters. The electronic couplings obtained from these fits are in good agreement with those values found previously. The extent of the solvent mediated superexchange mechanism was found to decrease significantly with an increase in the number and size of alkyl groups attached to the benzene core. In the second approach, the calculated $\Delta_r G$ and λ_o values were used to determine the electronic coupling at each temperature. The results show a steep decrease with increasing temperature of the D/A coupling in mesitylene and a less dramatic change in the other solvents that readily fit between the D and A groups. Molecular association could be the source of the decreased coupling at higher temperatures but further experimental work is necessary to determine this conclusively.

The Matyushov dipole−quadrupole solvation model is able to accurately reproduce and, in some cases predict, free energies in solvents ranging from nondipolar to highly dipolar. The model requires the vacuum free energy difference, $\Delta_{vac}G$, the difference in polarizability between the solute neutral and CT states, $\Delta\gamma'$, and an effective solute radius, R_{eff}. Calculations of these parameters may pose a significant problem, especially for large solutes. In addition, the use of the point dipole approximation for the charge redistribution in longer distance charge-transfer systems may be a limitation.[27] To conclude, the dipole−quadrupole model reproduces experimental rate data and provides insight into the solvent and temperature dependence of donor−acceptor electronic couplings.

Acknowledgment. This work was supported in part by the National Science Foundation (Grants CHE-9708351 (M.B.Z.) and CHE-941693 (D.H.W.)) We acknowledge numerous discussions with Dr. Dmitry Matyushov (University of Utah) and Prof. K. D. Jordan (University of Pittsburgh).

Appendix: Polynomial Forms of the Perturbation Integrals

$$I_{0s}^{(2)} = \frac{1}{r_0^3} + \frac{a(\rho^*)}{r_0^4} + \frac{b(\rho^*)}{r_0^5} + \frac{c(\rho^*)}{r_0^6}$$

$$I_6^{(2)} = \frac{a(\rho^*)}{r_0^5} + \frac{b(\rho^*)}{r_0^6} + \frac{c(\rho^*)}{r_0^7} + \frac{d(\rho^*)}{r_0^8}$$

$$I_{0s}^{(3)} = \frac{a(\rho^*)}{r_0^3} + \frac{b(\rho^*)}{r_0^4} + \frac{c(\rho^*)}{r_0^6}$$

$$I_{0s}^{(4)} = \frac{1}{r_0^9} + \frac{a(\rho^*)}{r_0^{10}} + \frac{b(\rho^*)}{r_0^{11}} + \frac{c(\rho^*)}{r_0^{12}}$$

$$I_{DQQ}^{(3)} = \frac{a(\rho^*)}{r_0^6} + \frac{b(\rho^*)}{r_0^7} + \frac{c(\rho^*)}{r_0^8} + \frac{d(\rho^*)}{r_0^9}$$

$$I_{DDQ}^{(3)} = \frac{a(\rho^*)}{r_0^5} + \frac{b(\rho^*)}{r_0^6} + \frac{c(\rho^*)}{r_0^7} + \frac{d(\rho^*)}{r_0^8}$$

$$J_1 = \frac{a(\rho^*)}{r_0^9} + \frac{b(\rho^*)}{r_0^{10}} + \frac{c(\rho^*)}{r_0^{11}}$$

In each case, r_0 is the reduced solute−solvent distance of closest approach, $r_0 = R_0/\sigma + 0.5$, and the functions $a(\rho^*)$, $b(\rho^*)$, etc. are fit to third-order polynomials over the reduced density, $\rho^* \equiv \rho\sigma^3$ such that

$$a(\rho^*) = a_0 + a_1\rho^* + a_2\rho^{*2} + a_3\rho^{*3}$$

These coefficients are listed in Table 6.

TABLE 6: Values of the Coefficients for the Polynomial Forms

	$I_{0s}^{(2)}$			$I_{0s}^{(3)}$			$I_{6}^{(2)}$				$I_{0s}^{(4)}$		
i	a_i	b_i	c_i	a_i	b_i	c_i	a_i	b_i	c_i	d_i	a_i	b_i	c_i
0	0.000	0.000	0.000	1.000	−0.563	0.031	1.000	0.000	0.000	0.000	0.000	0.000	0.000
1	1.935	−1.675	0.439	0.602	0.255	−0.256	0.586	1.062	−0.970	0.241	3.212	−2.580	0.608
2	−0.972	2.183	−1.051	−0.381	0.848	−0.263	−1.390	4.608	−4.134	1.194	2.862	−4.349	1.564
3	0.398	−0.831	0.465	−0.061	−0.107	0.098	0.776	−2.964	3.798	−1.393	−0.695	3.066	−1.447

	$I_{DQQ}^{(3)}$				$I_{DDQ}^{(3)}$				J_1		
i	a_i	b_i	c_i	d_i	a_i	b_i	c_i	d_i	a_i	b_i	c_i
0	0.208	0.000	−0.078	0.008	0.800	−0.500	0.000	0.031	0.774	0.021	1.140
1	0.936	−1.629	10.350	−6.712	0.365	1.652	−1.510	0.044	0.412	0.445	0.739
2	0.330	0.509	−20.530	13.990	−0.656	4.779	−7.378	3.770	0.885	0.372	0.751
3	−0.216	1.005	10.300	−7.512	0.179	−2.297	5.087	−2.928	0.565	0.361	0.410

TABLE 7: Individual Contributions to $\Delta_r G$ and λ_o (All Values in eV)[a]

Dipole Model Values for ΔG and λ ($\Delta_{vac}G = 0.326$)								Dipole−Quadrupole Model Values for ΔG and λ ($\Delta_{vac}G = 0.340$)								
T (K)	$\Delta_{dq,i}G^{(1)}$	$\Delta_i G^{(2)}$	$\Delta_{disp}G$	$\Delta_r G$	λ_p	λ_{ind}	λ_{disp}	λ_o	T (K)	$\Delta_{dq,i}G^{(1)}$	$\Delta_i G^{(2)}$	$\Delta_{disp}G$	$\Delta_r G$	λ_p	λ_{ind}	λ_{disp}	λ_o
								Benzene								
296	−0.407	−0.095	0.064	−0.112	0.000	0.095	0.003	0.099	296	−0.415	−0.031	−0.008	−0.115	0.163	0.031	0.000	0.194
312	−0.397	−0.086	0.062	−0.095	0.000	0.086	0.003	0.089	312	−0.399	−0.028	−0.008	−0.096	0.153	0.028	0.000	0.181
326	−0.388	−0.079	0.061	−0.081	0.000	0.079	0.003	0.082	326	−0.386	−0.026	−0.008	−0.080	0.144	0.026	0.000	0.170
342	−0.378	−0.072	0.059	−0.065	0.000	0.072	0.002	0.074	342	−0.371	−0.024	−0.008	−0.063	0.136	0.024	0.000	0.159
								Toluene								
296	−0.404	−0.097	0.089	−0.086	0.021	0.097	0.005	0.123	296	−0.379	−0.033	−0.012	−0.083	0.139	0.033	0.000	0.171
316	−0.391	−0.084	0.086	−0.063	0.019	0.084	0.005	0.108	316	−0.361	−0.028	−0.011	−0.061	0.127	0.028	0.000	0.156
331	−0.382	−0.076	0.084	−0.048	0.018	0.076	0.004	0.098	331	−0.348	−0.026	−0.011	−0.045	0.120	0.026	0.000	0.145
339	−0.377	−0.072	0.083	−0.040	0.017	0.072	0.004	0.093	339	−0.342	−0.024	−0.011	−0.037	0.116	0.024	0.000	0.140
347	−0.372	−0.068	0.082	−0.032	0.016	0.068	0.004	0.089	347	−0.335	−0.023	−0.011	−0.030	0.112	0.023	0.000	0.135
								Cumene								
296	−0.372	−0.097	0.088	−0.054	0.011	0.097	0.008	0.115	296	−0.347	−0.034	−0.010	−0.051	0.094	0.034	0.000	0.128
314	−0.362	−0.084	0.086	−0.035	0.010	0.084	0.007	0.101	314	−0.334	−0.030	−0.010	−0.034	0.087	0.030	0.000	0.117
324	−0.357	−0.078	0.084	−0.025	0.009	0.078	0.007	0.094	324	−0.328	−0.028	−0.010	−0.025	0.083	0.028	0.000	0.111
331	−0.354	−0.074	0.084	−0.018	0.009	0.074	0.006	0.090	331	−0.323	−0.026	−0.010	−0.019	0.081	0.026	0.000	0.107
345	−0.347	−0.067	0.082	−0.006	0.008	0.067	0.006	0.081	345	−0.314	−0.024	−0.010	−0.008	0.076	0.024	0.000	0.100
								TMB								
288	−0.382	−0.111	0.105	−0.062	0.026	0.111	0.011	0.148	288	−0.346	−0.039	−0.012	−0.057	0.094	0.039	0.000	0.134
298	−0.376	−0.104	0.103	−0.051	0.025	0.104	0.011	0.139	298	−0.339	−0.037	−0.012	−0.048	0.091	0.037	0.000	0.128
308	−0.370	−0.097	0.102	−0.040	0.023	0.097	0.010	0.131	308	−0.333	−0.034	−0.012	−0.040	0.088	0.034	0.000	0.123
318	−0.364	−0.091	0.100	−0.029	0.022	0.091	0.009	0.123	318	−0.328	−0.032	−0.012	−0.032	0.086	0.032	0.000	0.118
328	−0.359	−0.086	0.099	−0.020	0.021	0.086	0.009	0.116	328	−0.322	−0.030	−0.012	−0.024	0.083	0.030	0.000	0.113
								Mesitylene								
297	−0.365	−0.101	0.107	−0.033	0.001	0.101	0.011	0.114	297	−0.322	−0.036	−0.014	−0.032	0.081	0.036	0.000	0.117
303	−0.361	−0.097	0.106	−0.027	0.001	0.097	0.011	0.109	303	−0.318	−0.034	−0.013	−0.026	0.079	0.034	0.000	0.114
314	−0.356	−0.091	0.104	−0.016	0.001	0.091	0.010	0.102	314	−0.310	−0.032	−0.013	−0.016	0.075	0.032	0.000	0.107
324	−0.350	−0.085	0.103	−0.007	0.001	0.085	0.010	0.096	324	−0.304	−0.030	−0.013	−0.007	0.072	0.030	0.000	0.102
342	−0.341	−0.076	0.100	0.009	0.001	0.076	0.009	0.085	342	−0.293	−0.027	−0.013	0.008	0.067	0.027	0.000	0.094
								TIP								
260	−0.326	−0.117	0.097	−0.020	0.001	0.117	0.015	0.133	260	−0.303	−0.044	−0.010	−0.018	0.048	0.044	0.000	0.092
263	−0.325	−0.115	0.097	−0.017	0.001	0.115	0.014	0.130	263	−0.301	−0.044	−0.010	−0.016	0.047	0.044	0.000	0.091
278	−0.319	−0.104	0.095	−0.002	0.001	0.104	0.013	0.118	278	−0.294	−0.039	−0.010	−0.003	0.044	0.039	0.000	0.083
282	−0.317	−0.101	0.094	0.002	0.001	0.101	0.013	0.115	282	−0.292	−0.038	−0.010	0.000	0.043	0.038	0.000	0.081
								Acetonitrile								
250	−1.906	−0.038	0.051	−1.567	1.544	0.038	0.002	1.583	250	−1.083	−0.012	−0.006	−0.761	0.848	0.012	0.000	0.859
270	−1.868	−0.033	0.049	−1.526	1.517	0.033	0.001	1.552	270	−1.065	−0.010	−0.006	−0.741	0.837	0.010	0.000	0.847
300	−1.813	−0.027	0.046	−1.467	1.478	0.027	0.001	1.506	300	−1.039	−0.008	−0.006	−0.713	0.821	0.008	0.000	0.829
320	−1.776	−0.023	0.045	−1.429	1.452	0.023	0.001	1.477	320	−1.021	−0.007	−0.005	−0.694	0.810	0.007	0.000	0.817
340	−1.740	−0.020	0.043	−1.391	1.427	0.020	0.001	1.448	340	−1.004	−0.006	−0.005	−0.676	0.799	0.006	0.000	0.806
								Benzonitrile								
296	−1.864	−0.121	0.089	−1.570	1.444	0.121	0.007	1.572	296	−1.170	−0.041	−0.011	−0.882	0.892	0.041	0.000	0.933
312	−1.832	−0.109	0.088	−1.527	1.419	0.109	0.006	1.534	312	−1.154	−0.037	−0.011	−0.862	0.881	0.037	0.000	0.917
324	−1.807	−0.101	0.086	−1.496	1.400	0.101	0.006	1.507	324	−1.143	−0.034	−0.011	−0.847	0.872	0.034	0.000	0.906
342	−1.770	−0.090	0.084	−1.450	1.371	0.090	0.005	1.467	342	−1.125	−0.030	−0.010	−0.826	0.860	0.030	0.000	0.890

[a] TMB is 1,2,4-trimethylbenzene; TIP is 1,3,5-triisopropylbenzene.

References and Notes

(1) Matyushov, D. V.; Voth, G. A. *J. Chem. Phys.* **1999**, *111*, 3630. The formulation used in this manuscript includes solvent polarizability. We thank Dr. D. Matyushov for providing access to this form of the model.

(2) (a) Electron Transfer − From Isolated Molecules to Biomolecules. *Adv. Chem. Phys.*, Jortner, J., Bixon, M., Eds., (Wiley: NY **1999**) b) Barbara, P. F.; Meyer, T. J.; Ratner, M. A. *J. Phys. Chem.* **1996**, *100*, 13148. (c) Newton, M. D. *Chem. Rev.* **1991**, *91*, 767. (d) Closs, G. L.; Miller, J. R. *Science* **1988**, *240*, 440. (e) Marcus, R. A.; Sutin, N. *Biochimica et Biophysica Acta* **1985**, *811*, 265.

(3) (a) Newton, M. D. *Adv. Chem. Phys.* **1999**, *106*, 303. (b) Gray, H. B.; Winkler, J. R. *Annu. Rev. Biochem.* **1996**, *65*, 537. (c) Closs, G. L.; Calcaterra, L. T.; Green, N. J.; Penfield, K. W.; Miller, J. R. *J. Phys. Chem.* **1986**, *90*, 3673; (d) Jordan, K. D.; Paddon-Row, M. N. *Chem. Rev.* **1992**, *92*, 395.

(4) (a) Nitzan, A.; Mujica, V.; Davis, W. B.; Wasielewski, M. R.; Ratner, M. A. *J. Phys. Chem.* **1997**, *101*, 6158. (b) Häberle, T.; Hirsch, J.; Pöllinger, F.; Heitele, H.; Michel-Beyerle, M. E.; Anders, C.; Döhling, A.; Krieger, C.; Rückemann, A.; Staab, H. A. *J. Phys. Chem.* **1996**, *100*, 18269. (c) Heitele, H.; Pöllinger, F.; Häberle, T.; Michel-Beyerle, M. E.; Staab, H. A. *J. Phys. Chem.* **1994**, *98*, 7402. (d) Liu, J.; Schmidt, J. A.; Bolton, J. R. *J. Phys. Chem.* **1991**, *95*, 6924. (e) Ratner, M. A. *J. Phys. Chem.* **1990**, *94*, 4877. (e) Larsson, S. *Chem. Phys. Lett.* **1982**, *90*, 136. (f) Helms, A.; Heiler, D.; McLendon, G. *J. Am. Chem. Soc.* **1991**, *113*, 4325.

(5) (a) Liang, N.; Miller, J. R.; Closs, G. L. *J. Am. Chem. Soc.* **1989**, *111*, 8740. (b) Kumar, K.; Lin, Z.; Waldeck, D. H.; Zimmt, M. B. *J. Am. Chem. Soc.* **1996**, *118*, 243. (c) Kroon, J.; Oevering, H.; Verhoeven, J. W.; Warman, J. M.; Oliver, A. M.; Paddon-Row: M. N. *J. Phys. Chem.* **1993**, *97*, 5065. (d) Wasielewski, M. R.; Gaines, G. L. III,; O'Neill, M. P.; Svec, W. A.; Niemczyk, M. P.; Prodi, L.; Gosztola, D. in 'Dynamics and Mechanisms of Photoinduced Electron Transfer and Related Phenomena,' Mataga, N., Okada, T., Masuhara, H., Eds., Elsevier, 1992; p 87.

(6) (a) Read, I.; Napper, A.; Kaplan, R.; Zimmt, M. B.; Waldeck, D. H. *J. Am. Chem. Soc.* **1999**, *121*, 10976. (b) Han, H.; Zimmt, M. B. *J. Am. Chem. Soc.* **1998**, *120*, 8001. (c) Roest, M. R.; Verhoeven, J. W.; Schuddeboom, W.; Warman, J. M.; Lawson, J. M.; Paddon-Row, M. N. *J. Am. Chem. Soc.* **1996**, *118*, 1762.

(7) Vath, P.; Zimmt, M. B.; Matyushov, D. V.; Voth, G. A. *J. Phys. Chem. B* **1999**, *103*, 9130.

(8) McConnell, H. M. *J. Chem. Phys.* **1961**, *35*, 508.

(9) Gosztola, D.; Wang, B.; Wasielewski, M. R. *J. Photochem. Photobio. A.* **1996**, *102*, 71.

(10) Kumar, K.; Kurnikov. I. V.; Beratan, D. N.; Waldeck, D. H.; Zimmt, M. B. *J. Phys. Chem. A.* **1998**, *102*, 5529.

(11) Jortner, J. *J. Chem. Phys.* **1976**, *64*, 4860.

(12) (a) Marcus, R. A. *J. Phys. Chem.* **1989**, *93*, 3078. (b) Lilichenko. M.; Tittelbach-Helmrich, D.; Verhoeven, J. W.; Gould I. R.; Myers, A. B. *J. Chem. Phys.* **1998**, *109*, 10958. (c) Gould, I. R.; Noukakis, D.; Goodman, J. L.; Young, R. H.; Farid, S. *J. Am. Chem. Soc.* **1993**, *115*, 3830.

(13) Reynolds, L.; Frankland, S. J. V.; Horng, M. L.; Maroncelli, M. *J. Phys. Chem.* **1996**, *100*, 10337.

(14) Matyushov, D. V. *Chem. Phys.* **1996**, *211*, 47.

(15) Given the experimental rate constants, free energies, and the previous predictions of λ_i and ν, it was possible to compute the temperature dependence of λ_o at three values of the electronic coupling (ref 6a). The results gave nearly constant values of λ_o in every solvent but mesitylene. The origin of this temperature dependence in mesitylene is under investigation.

(16) Zeng, Y.; Zimmt, M. B. *J. Phys. Chem.* **1992**, *96*, 8395.

(17) Rehm, D.; Weller, A. Z. *Phys. Chem.* (*Munich*) **1970**, *69*, 183.

(18) Gubbins, K. E.; Joslin, C. G.; Gray, C. G. *Mol. Phys.* **1985**, *54*, 1117.

(19) (a) Matyushov, D. V.; Schmid, R. *J. Chem. Phys.* **1996**, *105*, 4729. This reference reports an erroneous value for the c_3 coefficient in the $I^{(2)}_{0s}$ polynomial form. Its value should be + 0.0983. See b) Matyushov. D. V.; Ladanyi, B. M. *J. Chem. Phys.* **1999**, *110*, 994.

(20) Ben-Amotz, D.; Willis, K. G. *J. Phys. Chem.* **1993**, *97*, 7736.

(21) Matyushov, personal communication.

(22) The values for the integral J_1 were provided by Dr Matyushov and fit to the polynomial form in the Appendix.

(23) Frisch, M. J.; Trucks, G. W.; Schlegel, H. B.; Scuseria, G. E.; Robb, M. A.; Cheeseman, J. R.; Zakrzewski, V. G.; Montgomery, J. A., Jr.; Stratmann, R. E.; Burant, J. C.; Dapprich, S.; Millam, J. M.; Daniels, A. D.; Kudin, K. N.; Strain, M. C.; Farkas, O.; Tomasi, J.; Barone, V.; Cossi, M.; Cammi, R.; Mennucci, B.; Pomelli, C.; Adamo, C.; Clifford, S.; Ochterski, J.; Petersson, G. A.; Ayala, P. Y.; Cui, Q.; Morokuma, K.; Malick, D. K.; Rabuck, A. D.; Raghavachari, K.; Foresman, J. B.; Cioslowski, J.; Ortiz, J. V.; Stefanov, B. B.; Liu, G.; Liashenko, A.; Piskorz, P.; Komaromi, I.; Gomperts, R.; Martin, R. L.; Fox, D. J.; Keith, T.; Al-Laham, M. A.; Peng, C. Y.; Nanayakkara, A.; Gonzalez, C.; Challacombe, M.; Gill, P. M. W.; Johnson, B. G.; Chen, W.; Wong, M. W.; Andres, J. L.; Head-Gordon, M.; Replogle, E. S.; Pople, J. A. *Gaussian 98*, revision A.4; Gaussian, Inc.: Pittsburgh, PA, 1998.

(24) The dipole moment of the charge transfer state was calculated assuming a point charge separation of 7.1 Å.

(25) Gubbins, K. E.; Gray, C. G.; Machado, J. R. S. *Mol. Phys.* **1981**, *42*, 817.

(26) (a) Vath, P.; Zimmt, M. B. *J. Phys. Chem. A* **2000**, *104*, 2626. (b) Cortés, J.; Heitele, H.; Jortner, J. *J. Phys. Chem.* **1994**, *98*, 2527.

(27) Zimmt, M. B. Unpublished results.